



GPU Nuclear, Inc.
U.S. Route #9 South
Post Office Box 388
Forked River, NJ 08731-0388
Tel 609-971-4000

January 6, 2000
1940-99-20662

U. S. Nuclear Regulatory Commission
Attn.: Document Control Desk
Washington, DC 20555

Subject: Oyster Creek Nuclear Generating Station
Facility License No. DPR-16
Docket No. 50-219
Response to Request for Additional Information re:
Proposed License Amendment for Spent Fuel Pool Expansion

Enclosure 1 to this letter provides our response to the request for additional information contained in the NRC letter dated November 22, 1999. In addition, enclosure 2 provides revised pages for the Licensing Report (Holtec Report HI-981983) attached to our June 18, 1999 license amendment request. The information on these pages is not proprietary. Pages 9-3 and 9-6 are revised to update accident dose results and radionuclide concentrations, respectively, as a result of subsequent analysis. The changes in radionuclide concentration result in slightly lower accident dose and, therefore, no increase in consequences. Page 3-4 is revised to change the lift rig load test duration from one hour to ten minutes as specified in ANSI 14.6 (1978).

Should further information be required, please contact Mr. Paul F. Czaya of our Nuclear Safety and Licensing Department at 609-971-4139.

Very truly yours,

A handwritten signature in black ink that reads "Sander Levin". The signature is fluid and cursive, written over a horizontal line.

Sander Levin
Acting Director
Oyster Creek

Enclosures

c: Administrator, USNRC Region I
USNRC Resident Inspector
Oyster Creek USNRC Project Manager

ADD 1

Enclosure 1

Question 1

You indicated in the Reference that the calculated seismic loading stresses in a fully loaded rack will not exceed those determined per Standard Review Plan (SRP) Section 3.8.4 which was used as a guide. With respect to your stress calculations using the DYNARACK computer code presented in Chapter 6 of the Reference:

- (a) Explain how the simple stick model used in the dynamic analyses can represent accurately and realistically the actual complicated nonlinear hydrodynamic fluid-rack structure interactions and behavior of the fuel assemblies and the box-type rack structures; and discuss whether or not a finite element (FE) model with 3-D plate, beam and fluid elements together with appropriate constitutive relationships would be a more realistic, accurate approach to analyze the fluid-structure interactions in contrast to the simple stick model.
- (b) Provide the results of any prototype experimental study that verifies the correct or adequate simulation of the fluid coupling utilized in the numerical analyses for the fuel assemblies, racks and walls. If no such experimental study is available, explain how the current level of DYNARACK code verification is adequate for engineering application without further experimental verification work.
- (c) Provide the physical dimensions of the racks, and the gaps between the racks and the gaps between the racks and the spent fuel pool (SFP) walls.
- (d) Demonstrate that the artificial seismic ground motion time histories used in the analyses satisfy the power spectral density (PSD) requirement of SRP 3.7.1.

Response to Question 1 (a)

The analysis of the underwater kinematics of a highly nonlinear structure, such as a spent fuel rack loaded with freestanding spent nuclear fuel, is a highly complex problem. An unconditionally convergent and stable solution is obtained using a two step process, wherein the kinematics of the rack and the global forces are computed using a numerically robust code based on the "component element method of simulation", viz., DYNARACK.

DYNARACK, developed in the late 1970s and continuously updated since that time to incorporate technology advances such as multi-body fluid coupling, is a code based on the Component Element Method (CEM). The chief merit of CEM is its ability to simulate friction, impact, and other nonlinear dynamic events with accuracy. The beam characteristics of the rack,

including shear, flexure, and torsion effects, are appropriately modeled in DYNARACK using the classical CEM "beam spring". However, the rack is not rendered into a "stick" model. Rather, each rack is modeled as a prismatic 3-D structure with support pedestal locations and the fuel assembly aggregate locations set to coincide with their respective Center of Gravity axes. The potential rattling between the fuel and storage cells is simulated in exactly the same manner as it would be experienced in nature: namely, impact at any of the four facing walls followed by rebound and impact at the opposite wall. Similarly, the rack pedestals are allowed to lift off, or slide, as the instantaneous dynamic equilibrium would dictate throughout the seismic event. The rack structure is permitted to undergo overturning, bending, twist, and other dynamic motion modes as determined by the interaction between the seismic inertia, impact, friction, and fluid coupling forces. Hydrodynamic loads, which can be significant, are included in a comprehensive manner.

The results from DYNARACK enable primary stresses in supports, welds, etc. to be directly computed. Detailed finite element models are constructed to evaluate the cell structure above the support pedestals. Evaluations are performed using both beam, and plate and shell, criteria as appropriate.

Response to Question 1 (b)

A key ingredient in the Whole Pool Multi-Rack (WPMR) analysis is quantification of the hydrodynamic coupling effect that couples the motion of every rack with every other rack in the pool. In 1987, Dr. Burton Paul (Professor Emeritus, University of Pennsylvania) developed a fluid mechanics formulation using Kelvin's recirculation theorem which provided the fluid coupling matrix ($2n \times 2n$ for a pool containing n racks). For example, with reference to Attachment 1.1, where an array of N ($N = 13$) two-dimensional bodies (each with two degrees of freedom) is illustrated, the dynamic equilibrium of the i -th mass in the x -direction can be written as:

$$[m_i + M_{ii}] \ddot{x}_i + \sum_{j=1}^N [M_{ij} \ddot{x}_j + N_{ij} \ddot{y}] = Q_{xi}(t)$$

In the above equation, m_i is the mass of body i ($i = 1, 2, \dots, N$), and \ddot{x}_i is the x -direction acceleration vector of body i . M_{ij} and N_{ij} denote the "virtual" mass effects of body j on body i in the two directions of motion. The second derivative of y with respect to time represents the acceleration in the y -direction.

The terms M_{ij} and N_{ij} are functions of the shape and size of the bodies, the container boundary, and, most importantly, the size of the inter-body gaps. M_{ij} and N_{ij} are analytically derived coefficients. Q_{xi} represents the generalized force that may be an amalgam of all externally

applied loads on the mass i in the x -direction. The above equation for mass i in x -direction translational motion is then written for all degrees of freedom and for all masses. The resulting second order, matrix differential equation contains a fully populated mass matrix. (In contrast, dynamic equations without multi-body fluid coupling will have only diagonal non-zero terms).

Dr. Paul's formulation is documented in a series of four reports written for PG&E in 1987, which were previously submitted to the NRC. The Paul multi-body fluid coupling theory conservatively assumes the flow of water to be irrotational (inviscid) and assumes that no energy losses, due to form drag, turbulence, etc., occur. The NRC reviewed this formulation in the course of their audit of the Diablo Canyon rerack (ca. 1987) and subsequently testified in the ASLB hearings on this matter.

While the ASLB, NRC, and Commission consultants, Brookhaven National Laboratory and Franklin Research Center, all endorsed the Paul multi-body fluid coupling model as an appropriate and conservative construct, the theory was still just a theory. Recognizing this perceptual weakness, Holtec and Northeast Utilities undertook an experimental program in 1988 to benchmark the theory. The experiment consisted of subjecting a scale model of racks, from one to four at one time in the tank, to a two-dimensional excitation on a shake table at a QA qualified laboratory in Waltham, Massachusetts.

The Paul multi-body coupling formulation, coded in QA validated preprocessors to DYNARACK, was compared to the test data. Over 100 separate tests were run. The experimental benchmark work validated Paul's fluid mechanics model and showed that the theoretical model is consistently bounded by the test data. This experimentally verified multi-body fluid coupling technology is the central underpinning of the DYNARACK WPMR solution that has been employed in every license application since Chinshan (1989). The DYNARACK 3-D WPMR solution has been found to predict greater rack displacements and rotations than the previously used 3-D single rack results. The proprietary report on Holtec's fluid coupling experiments (HI-88243) was provided to the NRC on the Waterford 3 docket recently.

In summary, the WPMR analysis utilizes a fluid coupling formulation that is theoretically derived, without empiricism, and experimentally validated. The assumptions built in to the DYNARACK formulation are aimed to demonstrably exaggerate the response of all racks in the pool simulated in one comprehensive model.

Response to Question 1 (c)

The physical dimensions of the racks are provided in the table below.

Rack I.D.	No. of Cells		Envelope Size, in		Height, in
	N-S Dir.	E-W Dir.	N-S Dir.	E-W Dir.	
L	12	8	73.647	49.223	176.188
M	12	9	73.647	55.329	176.188
N	11	8	67.541	49.223	176.188
P	11	13	67.541	79.753	176.188

Attachment 1.2 shows the gaps between the racks and the gaps between the racks and the spent fuel pool (SFP) walls.

Response to Question 1 (d)

Two sets of artificial time histories were used in the analyses: a Safe Shutdown Earthquake (SSE) and an Operating Basis Earthquake (OBE). Both sets were derived from the Reactor Building response spectra at El 75'-3" developed by EQE. These spectra are contained in EQE Report entitled "Design Criteria for Soil-Structure Interaction Analysis of the Reactor/Containment Building at GPUN Oyster Creek Nuclear Generating Station", dated June 1993. They were approved for use by the NRC on February 23, 1995. See letter A. W. Dromerick to J. J. Barton, "Review and Evaluation of the Soil-Structure Interaction Analysis and Approach Proposed for Generation of In-Structure Spectra (TAC NO. M69467)." Attachment 1.3 presents Figures 2-15, 2-16 and 2-17 from the EQE Report, which show the comparison of the PSDs from the time histories to the targets. As discussed in the report, these figures demonstrate that the time histories used are compliant with the requirements of SRP 3.7.1.

The SSE time histories for use in the DYNARACK analyses were also developed by EQE. Attachment 1.4 presents Section 7.0 and Figures 7-1 through 7-6 from the EQE calculation which demonstrate that the time histories derived contain the correct energy distribution with respect to frequency. The OBE time histories, which were generated by Holtec International, also meet the PSD requirements of SRP 3.7.1. Attachment 1.5 contains figures, which provide a comparison of the PSD curves associated with the generated time histories and the PSD curves associated with the design basis response spectra. These figures clearly show that the generated PSD curves envelop the target curves over the entire frequency range.

Question 2

You indicated in the Reference that the design conditions described in SRP 3.8.4 and American Concrete Institute (ACI) Code 349-80 were used as guidance in the calculations of SFP capacity. With respect to the SFP capacity calculations using ANSYS computer code presented in Chapter 8 of the Reference:

- (a) Provide the physical dimensions of the reinforced concrete slab and walls, liner plate and the details of liner anchorage; also provide the material properties used in the analysis.
- (b) Provide the mesh used in the analysis; describe the boundary conditions and indicate them in the mesh.
- (c) Describe the applied loading conditions including magnitudes, and indicate their locations in the mesh.
- (d) Explain how the interface between the liner and concrete slab is modeled, and also, how the liner anchors are modeled; explain how such modeling accurately represents the real structural behavior.
- (e) Provide the calculated governing factors of safety in a tabular form for the axial, shear, bending and combined stress conditions in the spent fuel pool.

Response to Question 2 (a)

The inside (plan) dimensions of the pool are 27'-0" (North-South) by 39'-0" (East-West). The pool depth, which is measured from the top of the liner (EL. 80'-6") to the top of the pool curb (EL. 119'-7"), is 39'-1".

The contents of the pool are supported by a two-way, reinforced concrete slab and the underlying beams. The minimum thickness of the slab is 54 inches, excluding the grout layer. The SFP walls to the north and to the east are 6 feet thick. The thickness of the west wall is 6 feet, below elevation 95'-3", and is reduced to 54 inches above elevation 95'-3", where the new fuel dry storage vault is located. The south wall of the pool is an integral part of the concrete reactor shield, and it has a minimum thickness of 6 feet. The walls are braced from the outside by several intermediate floor slabs.

A fully welded, stainless steel liner covers the interior surface of the pool. The floor consists of an array of 1/4" thick plates, and the wall covering is fabricated from 1/8" thick material. The liner anchorage in the floor consists of a series of 6" x 6" x 1/4" beams, which are embedded in

the grout layer beneath the liner. These beams lie in the East-West direction, and they are spaced approximately every 2 feet. The beams are anchored to the slab by 3/4" diameter bolts. The liner is continuously welded to the embedment beams along the plate splices.

The material properties, which are used in the analysis, are:

Concrete

Compressive Strength (f_c')	3,000 psi
Modulus of Elasticity	3.12×10^6 psi
Poisson's Ratio	0.167
Shear Modulus	1.34×10^6 psi
Maximum Compressive Strain	0.003

Steel Reinforcement

Modulus of Elasticity	29.0×10^6 psi
Yield Stress	40,000 psi

Liner Plate/Anchorage (ASTM A240-304L)

Modulus of Elasticity	27.6×10^6 psi
Poisson's Ratio	0.30
Yield Stress	25,000 psi
Ultimate Stress	70,000 psi

Liner Welds

Nominal Tensile Strength	70,000 psi
--------------------------	------------

Response to Question 2 (b)

The finite element model encompasses the entire area of interest, i.e., the reinforced concrete slab, its three supporting beams, and the SFP walls. Attachment 2.1 provides an isometric view of the mesh. The interaction of the spent fuel pool with the rest of the Reactor Building is simulated by appropriate boundary conditions. Attachment 2.2 indicates the type and locations of the boundary conditions.

The specific boundary conditions are:

- All sixteen nodes that lie on the southern edge of the slab, where the slab connects with the reactor shield, are completely fixed.
- The end nodes of the reinforced concrete beams are simply supported.
- The slab node that is located at the intersection of column lines RC and R6 is simply supported to simulate the underlying column.
- Two additional slab nodes are vertically constrained to simulate the concrete gussets beneath the slab.

Response to Question 2 (c)

The applied load conditions are dead, thermal, seismic, and cask drop loads.

Dead Load

The dead loads acting on the SFP concrete slab consist of the self weight of the concrete structure, the weight of the fully loaded spent fuel racks and cask in the pool, and the weight of the pool water. All the loads contained in this category are statically applied loads. The magnitude of the loads used in the analysis are summarized below:

The self weight of the concrete structure is calculated based on a density of 150 lb/ft³.

The total dead weight of the fully loaded spent fuel racks is 2,440,910 lbf. The weight associated with each individual rack pedestal is converted into a concentrated mass, and then the concentrated masses are assigned to the nearest slab nodes. Under an applied gravitational load, these masses simulate the total dead weight of the spent fuel racks. The dead weight of the cask (200,000 lbf) is applied to the slab in a similar fashion.

Hydrostatic water pressure varies linearly along the height of the walls. Based on a water density of 62.4 lb/ft^3 and a conservative pool depth of 40 feet, the hydrostatic water pressure acting on the slab is 17.33 lb/in^2 .

Thermal Load

Two different thermal loads are investigated. Thermal gradients of 25°F and 60°F are applied across the slab thickness to simulate the summer (poolside cooler) and winter (poolside warmer) conditions, respectively. The temperatures applied to the structural elements are based on the extreme limits of the normal operating condition.

Seismic Loads

Two levels of seismic events are considered in the analysis: the operating basis earthquake (OBE) and the safe shut down earthquake (SSE). For each earthquake, the loads are subdivided into the following three categories:

(i) Structural Seismic Loads

The inertial load of the reinforced structure is computed by multiplying the dead weight of the concrete with the corresponding zero period acceleration (ZPA) in the vertical direction. The ZPA values for the OBE event and the SSE event, which are used in the structural analysis, are:

Vertical ZPA for OBE 0.100g

Vertical ZPA for SSE 0.190g

This load is applied to the model as an acceleration load.

(ii) Hydrodynamic Load

The vertical movement of the water mass, due to the vertical component of the ground acceleration, induces time dependent wall and floor pressures. This component of the seismic load is conservatively computed by multiplying the hydrostatic water pressure with the corresponding ZPA value.

For the numerical analysis, this load is obtained by applying a scale factor to the hydrostatic pressure load.

(iii) Rack/Cask Seismic Load

The rack and cask vertical seismic loads are computed by multiplying the concentrated masses (see description under Dead Load) with the corresponding ZPA values.

This load is applied to the model as an inertia load (i.e., mass times acceleration).

Cask Drop Load

The cask drop load is applied as an equivalent static load of 1560 kips, which is the design basis value for the Cask Drop Protection System installed in the OCNGS pool. The load is equally divided among the sixteen nodes located in the cask area.

Response to Question 2 (d)

The liner in the Oyster Creek pool is assembled from Austenitic stainless steel plates which are seam welded along the contiguous edges of the plates resulting in a sealed container geometry to hold water. These edges are located over the embedded beams and the welds not only weld the plates together, they also weld the plates down to the beams. The seam weld lines are, therefore, anchor locations. The integrity analysis of the pool liner consists of the following evaluations:

- (i) Insure that the in-plane stresses in the liner during the seismic event would not cause rupture of the liner from a single load application.**
- (ii) Insure that repetitive load during a seismic event will not lead to fatigue failure of the liner. One SSE and twenty (20) OBEs occurring in sequence is the design basis.**

To evaluate the stress field in the liner, it is modeled as a 2-D plate anchored at the weld seam locations. A bounding geometry was utilized wherein the anchor lines are nearest to the pedestal location.

Response to Question 2 (e)

The following table summarizes the governing (minimum) safety factors in the spent fuel pool structure.

Structural Element [†]	Bending		Shear	
	N-S Direction	E-W Direction	N-S Direction	E-W Direction
Beam RD	2.06	-	2.96	-
Beam RE	1.19	-	2.92	-
Beam R6	-	1.06	-	1.43
Slab	1.45	1.71	1.11	1.09

[†] Attachment 2.1 shows the locations of the structural elements.

Question 3

The maximum bulk pool temperature during a partial core discharge (shown as Case (i) in Table 5.8.1 and Figure 5.8.1 of the Reference) exceeds 150°F which is the allowable ACI Code 349 limit for concrete temperature for normal operation or any other long term period. Provide technical justifications for exceeding the allowable temperature of 150°F. Also describe details of the SFP structural analysis including the material properties (i.e., modulus of elasticity, shear modulus, poisson's ratio, yield stress and strain, ultimate stress and strain, compressive strength) used in the analysis for the reinforced concrete slab walls, liner plate, welds and anchorages.

Response to Question 3

Two partial core discharges are analyzed in Chapter 5 of the Reference. The two cases differ by the available spent fuel pool cooling capacity. Case (ii) represents a partial core discharge under normal operating conditions, wherein the spent fuel pool is cooled by a large capacity (12.2×10^6 Btu/hr) augmented heat exchanger operating with one pump. The maximum bulk pool temperature for this case is 114.10°F (Table 5.8.1 of the Reference), which is well below the ACI-349 allowable limit for concrete temperature.

If both pumps to the augmented heat exchanger are unavailable during a partial core discharge, then the spent fuel pool is cooled by two smaller shell-and-tube heat exchangers, which have a total cooling capacity of 5.5 million Btu/hr. This scenario, which is identified in the Reference

1940-99-20662

Page 11 of 11

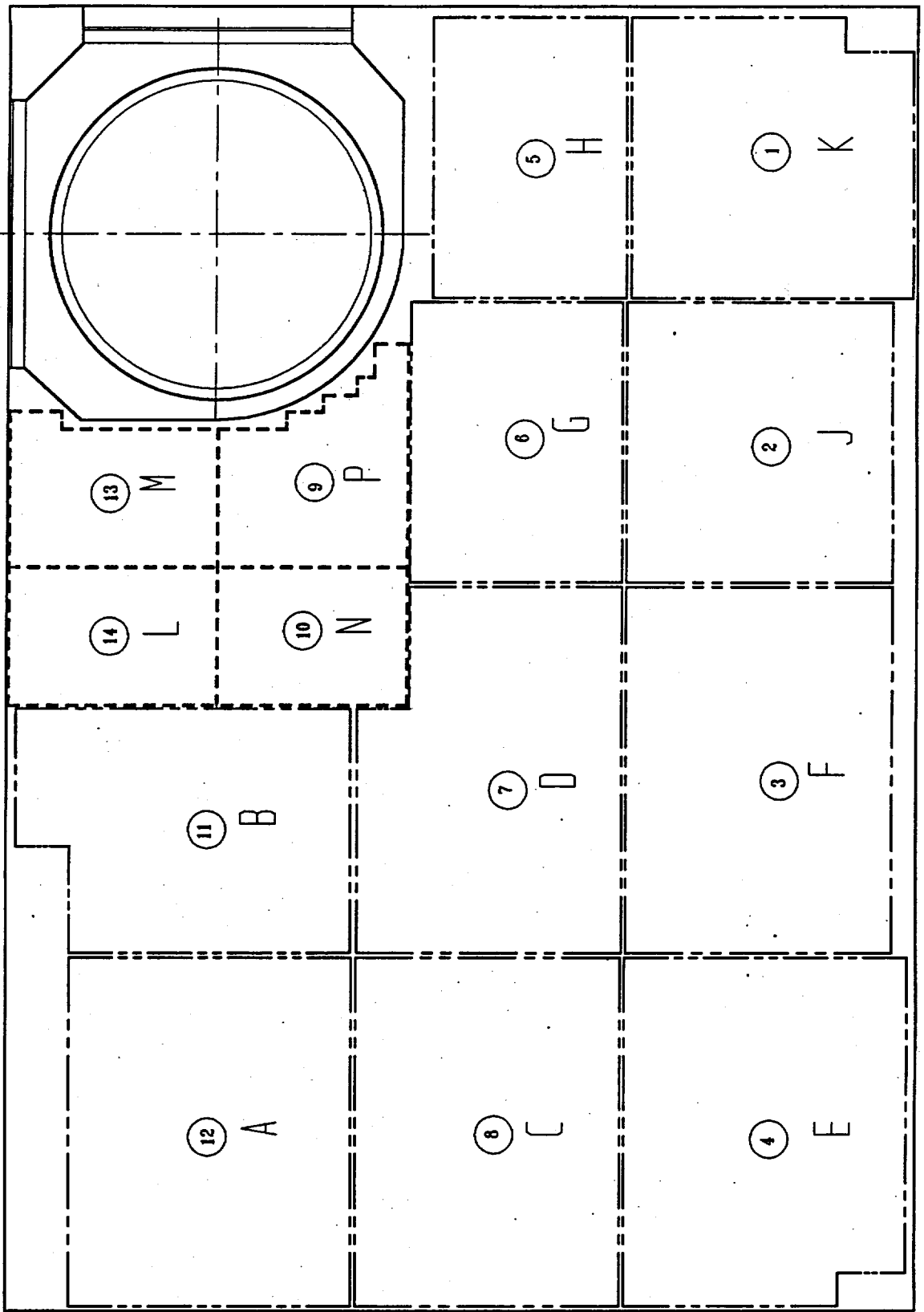
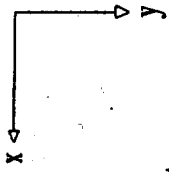
Enclosure 1

as Case (i), is an abnormal condition. Calculations predict that under these circumstances the bulk pool temperature rises to 168.35°F (Table 5.8.1 of the Reference). Since this is an abnormal condition and the decay heat generated by the spent nuclear fuel decays exponentially, SFP temperature would remain above 150°F for approximately 25 days, based on Figure 5.8.1. However, Oyster Creek Technical Specification 5.3.1.D limits bulk fuel pool water temperature to 125°F. Plant procedures require core discharge activities to cease when pool temperature reaches 115°F. Measures will be taken to return the augmented system to service or recently irradiated fuel assemblies could be returned to the reactor vessel in order to prevent exceeding the Technical Specification limit. While Case (i) was evaluated to conform with SRP guidelines, the condition is not believed to be credible.

For the SFP structural analysis, the material properties are consistent with normal operating temperatures, which are below 150°F. See Response to Question 2(a) for a complete listing of the material properties.

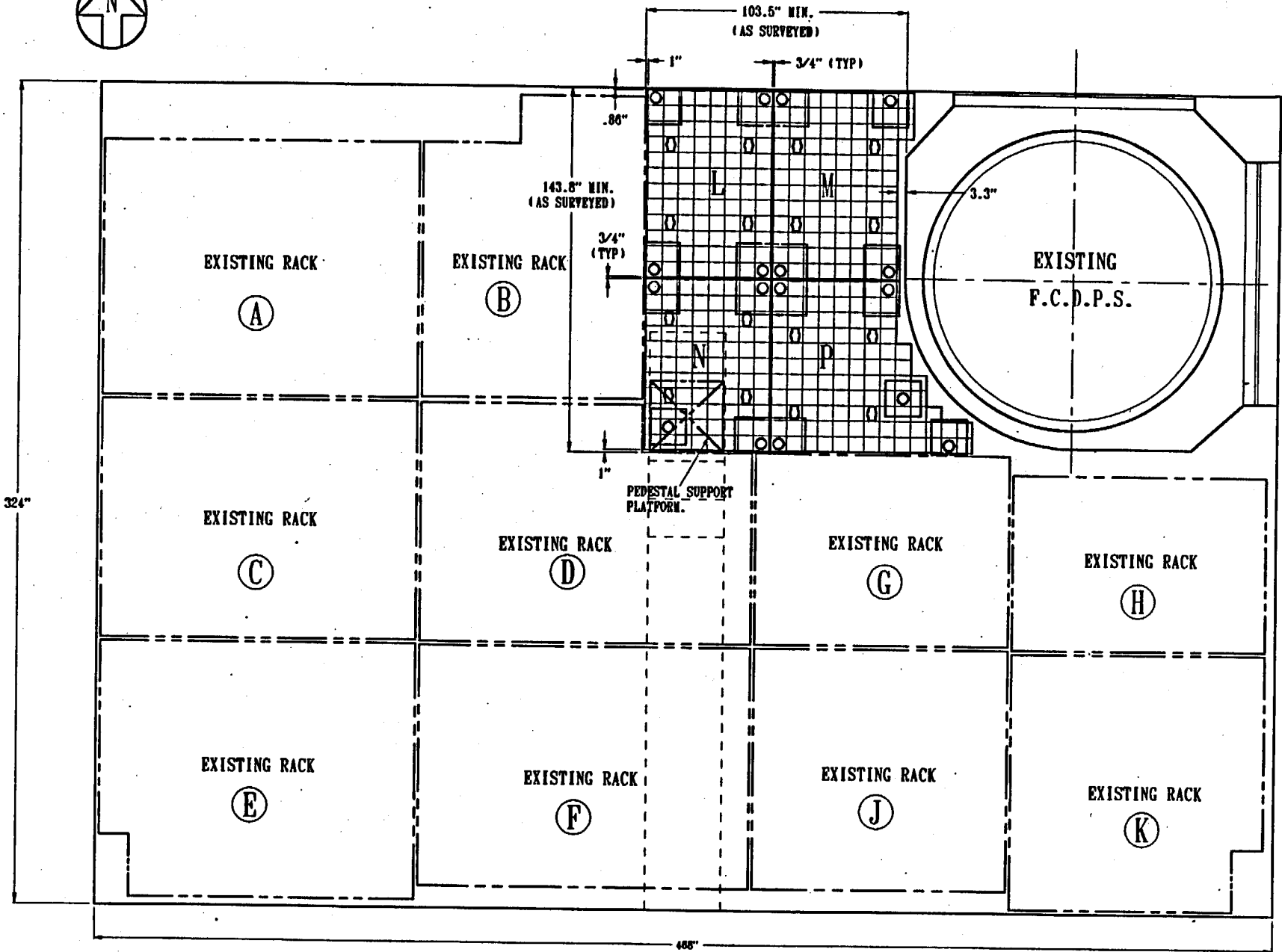
Attachment 1.1

Two Dimensional Array of N Bodies (N=13)



Attachment 1.2

**OCNGS Spent Fuel Pool Rack Layout
W/Gap Dimensions**



Attachment 1.3

**OCNGS Site Specific Time Histories
PSD Functions Vs Targets**

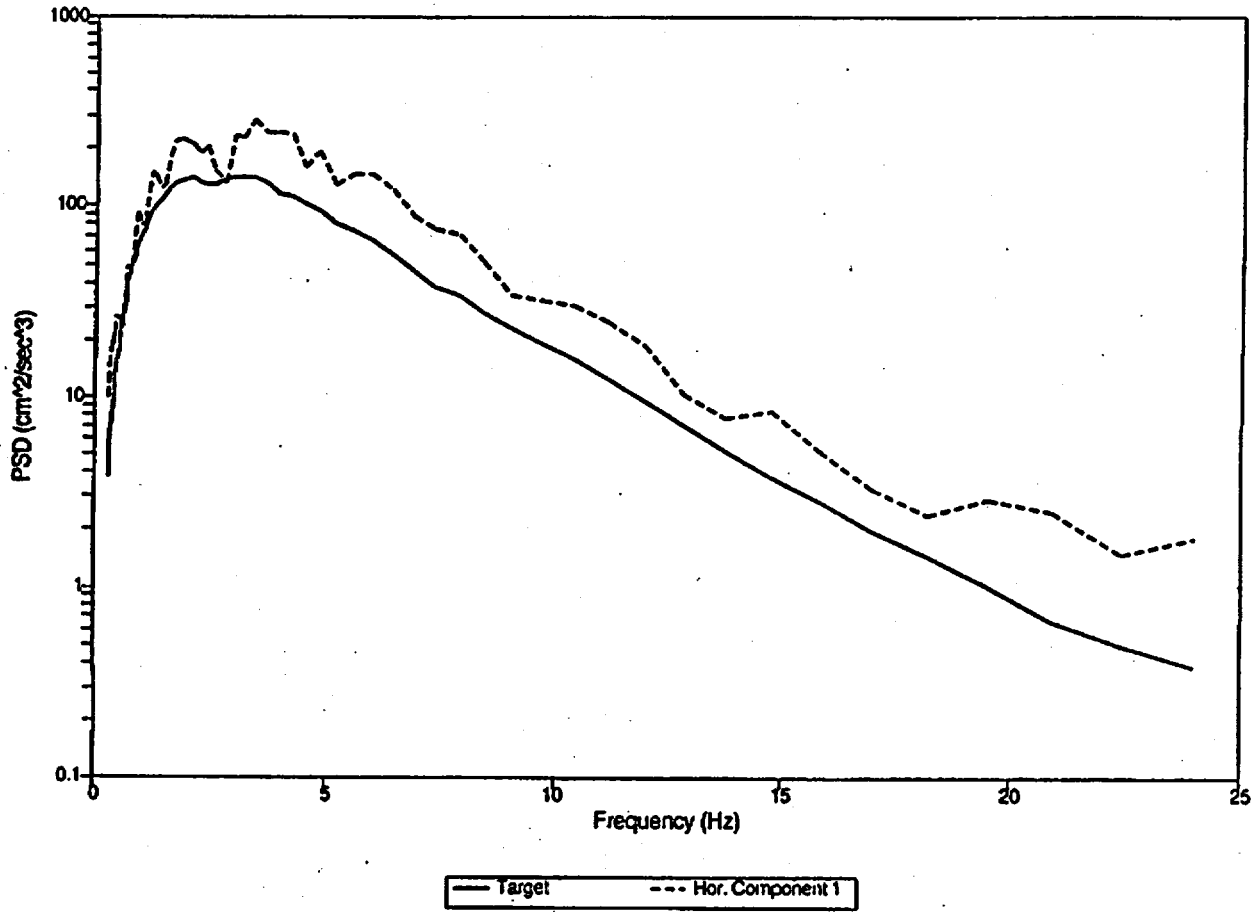


Figure 2-15: Comparison of PSD Functions, Horizontal Component 1, Artificial Time History vs. Target

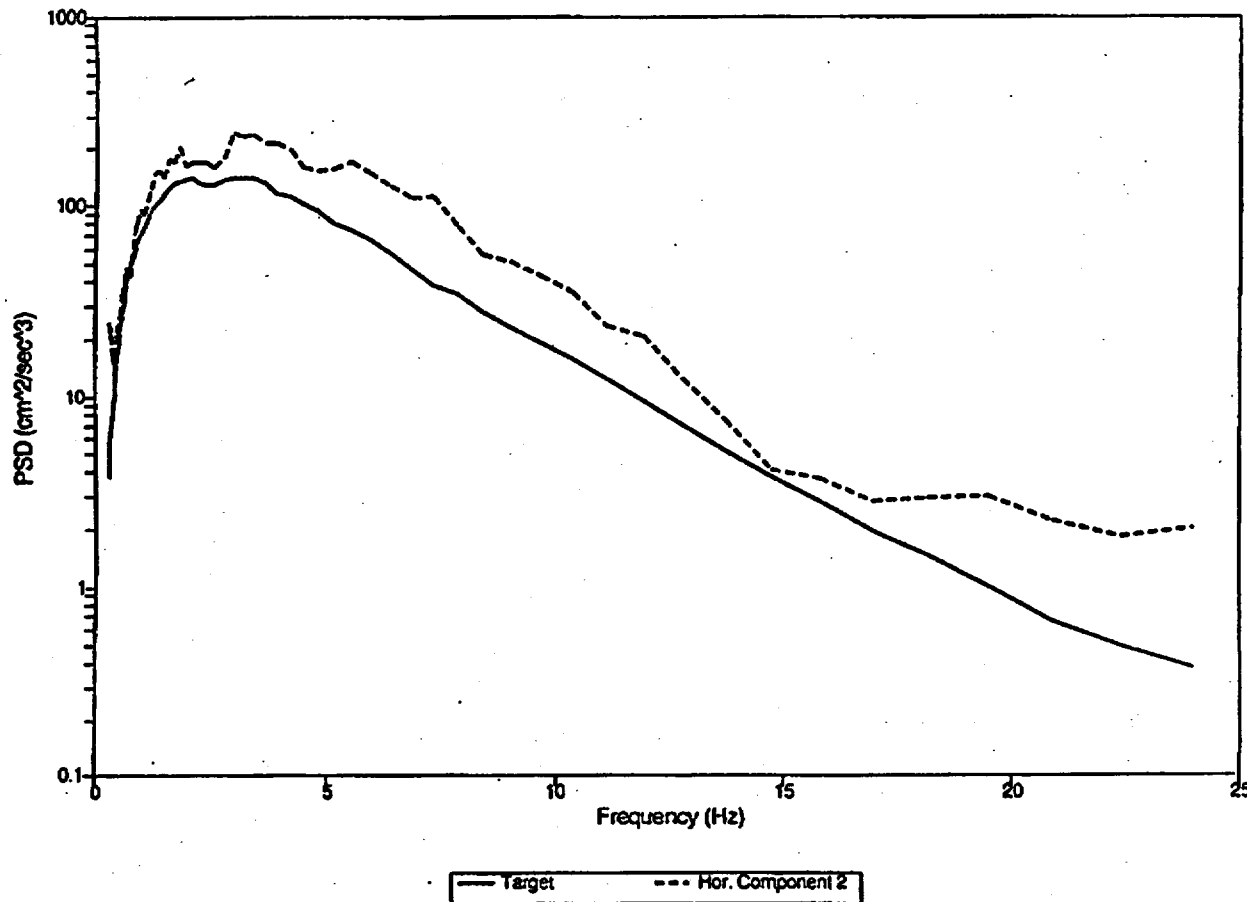


Figure 2-16: Comparison of PSD Functions, Horizontal Component 2, Artificial Time History vs. Target

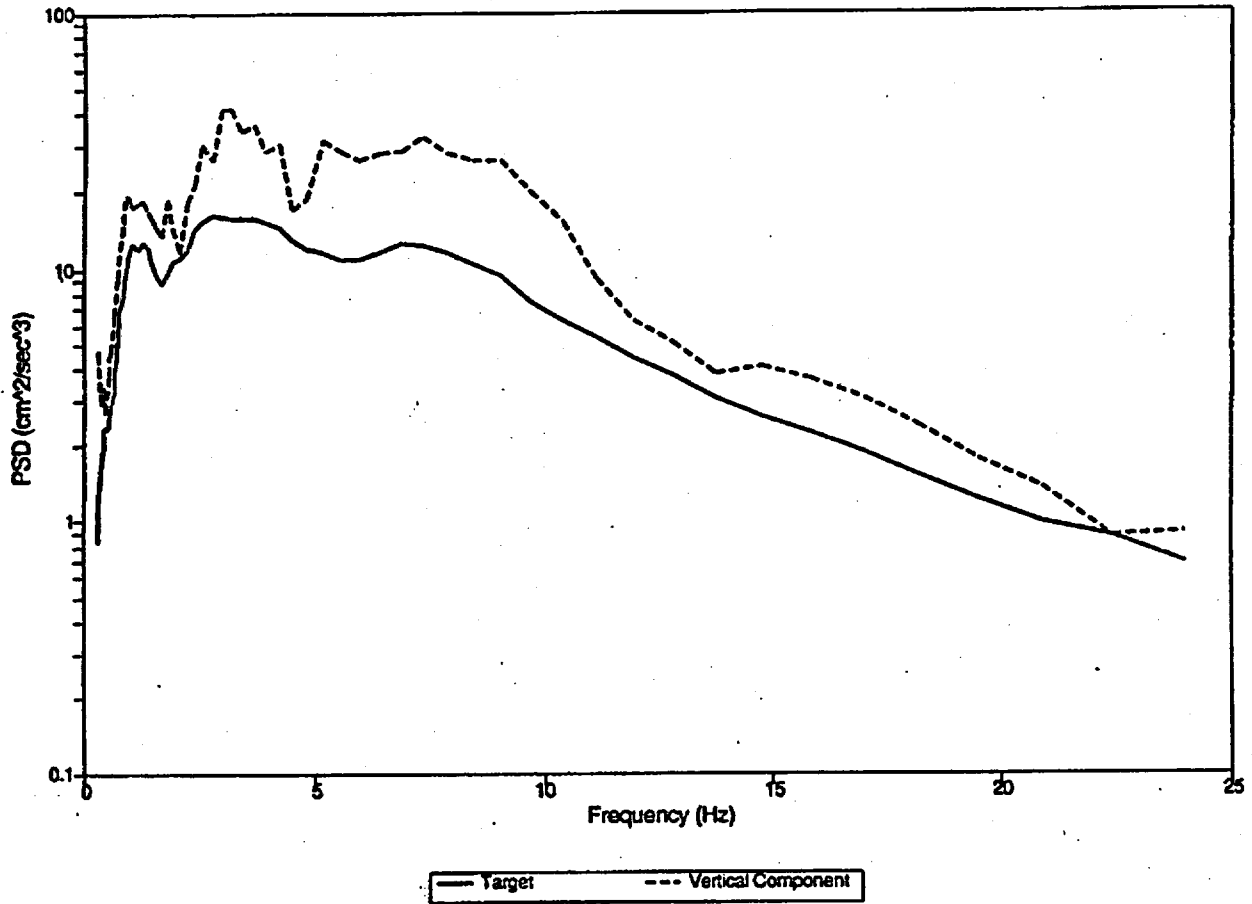


Figure 2-17: Comparison of PSD Functions, Vertical, Artificial Time History vs. Target

Attachment 1.4

**OCNGS SSE Time Histories at El. 75'-3"
PSD Functions Vs Targets**



EQE INTERNATIONAL

SHEET NO. 36JOB NO. 100028.01 JOB OCNGS Time Histories for Fuel PoolBY APA DATE 4/7/97CALC. NO. 100028C01R0 SUBJECT Development of Artificial Time HistoriesCHK'D DDD DATE 1/2/97

7.0 Verification of Power Spectra Density

To verify that "on average" the time histories have the correct distribution of energy with frequency, their power spectral density functions were calculated. This parameter is defined as:

$$\text{PSD}(\omega) = |F(\omega)|^2 / T_{SM}$$

Where $F(\omega)$ is the Fourier transform of the acceleration time history and T_{SM} is an estimate of the strong motion duration of the time history. For the calculation of the power spectral density functions the strong motion duration was estimated as the time between 90% and 5% of the energy. This resulted in:

$$T_{SM} \text{ (NS)} = 10.93 \text{ seconds}$$

$$T_{SM} \text{ (EW)} = 10.82 \text{ seconds}$$

$$T_{SM} \text{ (Vert)} = 11.92 \text{ seconds}$$

The power spectral density functions were smoothed by an averaging process in a frequency window of $\pm 20\%$.

The "raw" and smooth power spectral density functions are shown in Figures 7-1 to 7-6. There, it is shown that the generated horizontal time histories have the energy concentrated in the 3 to 4 Hz range and practically no energy after 8 to 10 Hz. The vertical time history has a large amount of energy in the 3 to 4 Hz range but also has energy between 4 and 20 Hz. This is consistent with the target floor response spectra and with the characteristics of the dynamic response of the reactor building.

Figure 7-1: Raw Power Spectral Density Function - North-South Component

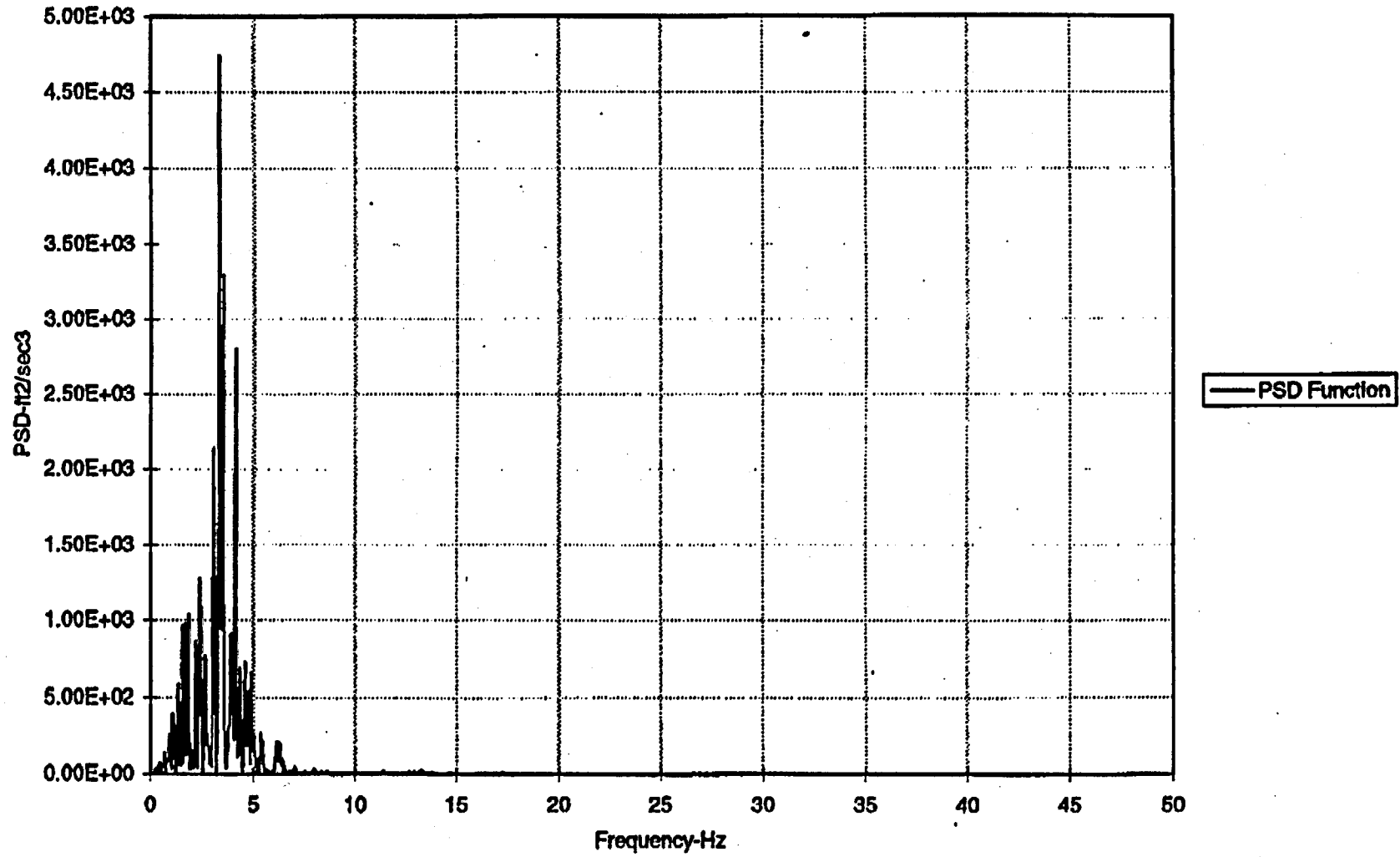


Figure 7-2: Smooth Power Spectral Density Function - North-South Component

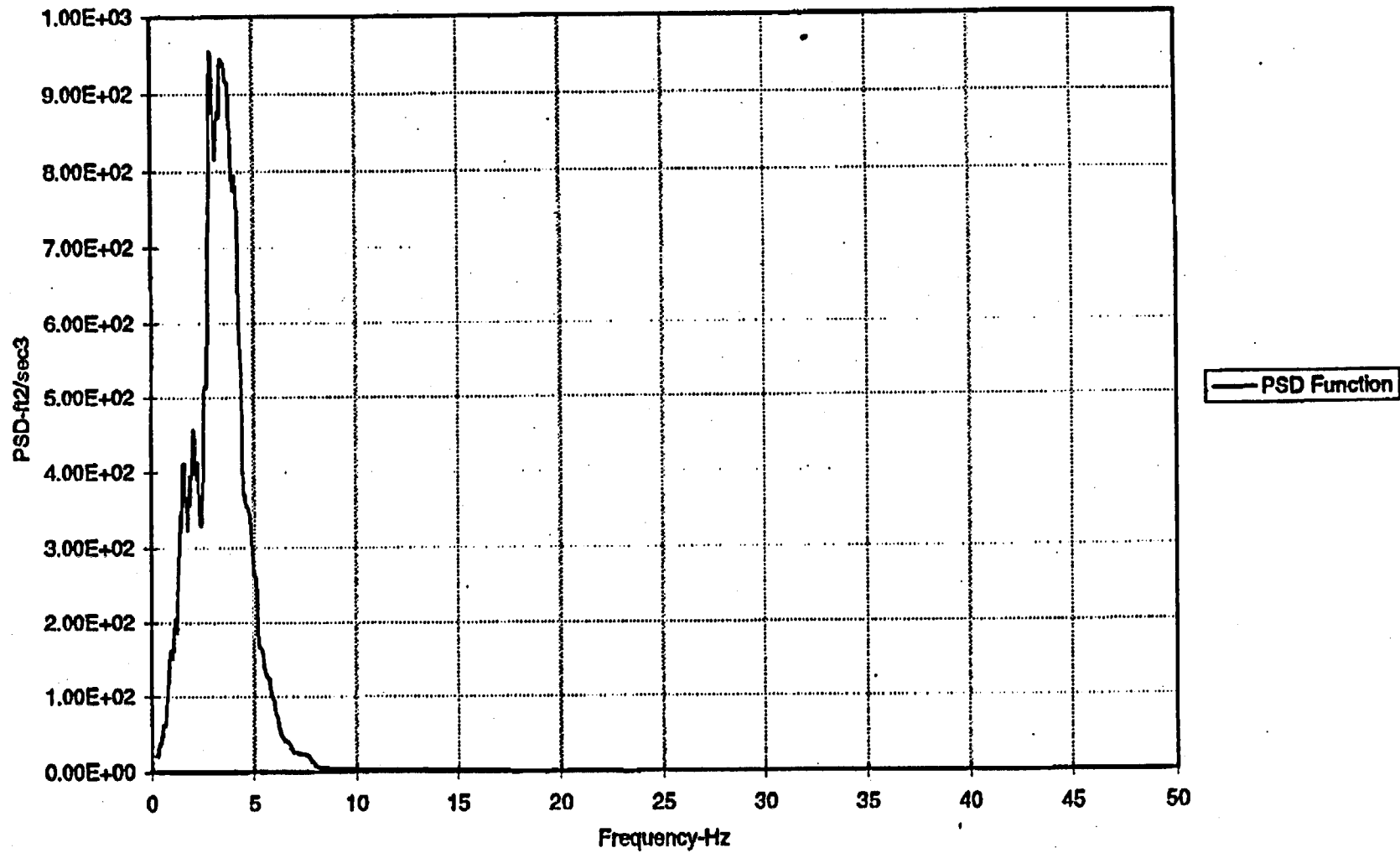


Figure 7-3: Raw Power Spectral Density Function - East-West Component

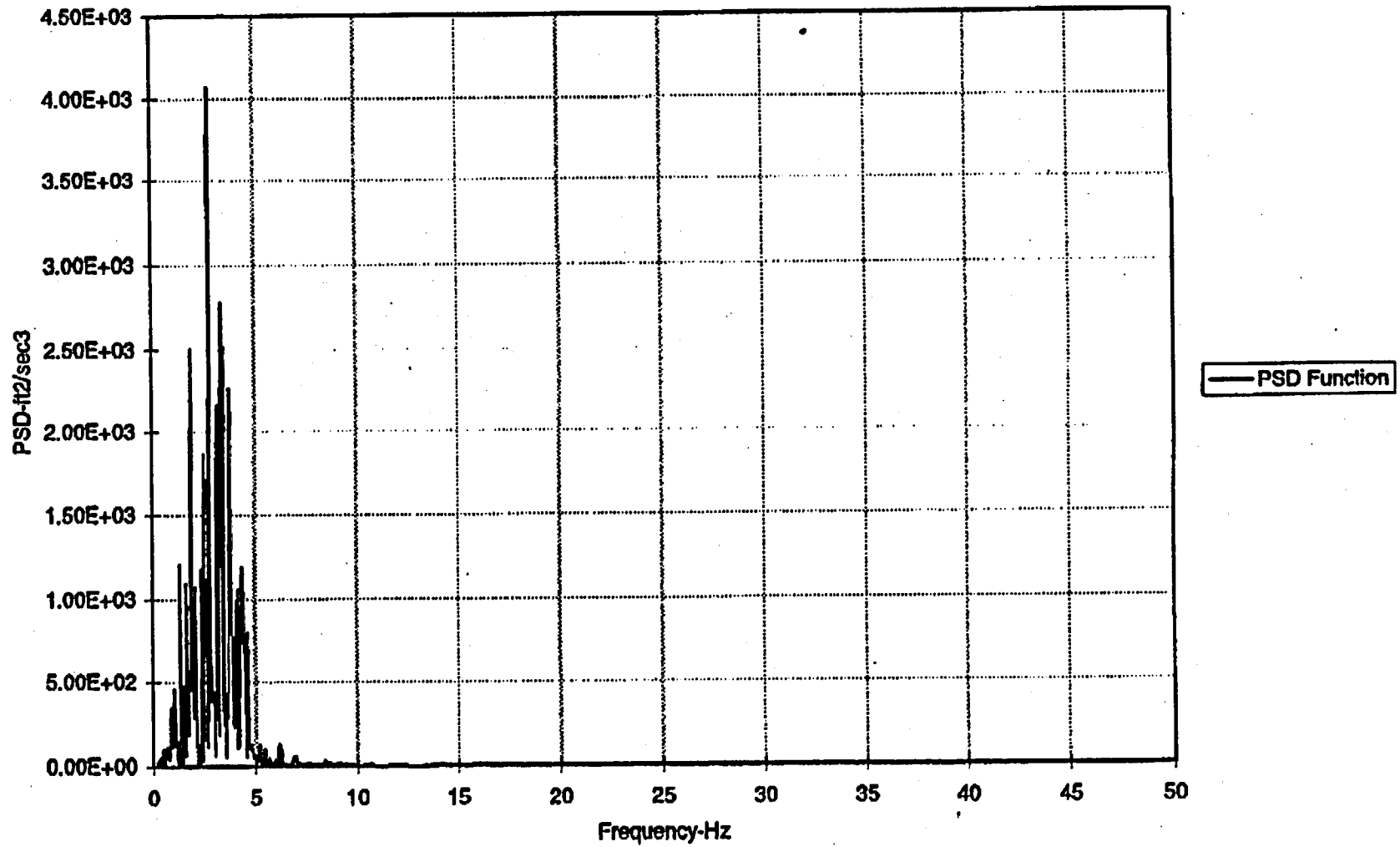


Figure 7-4: Smooth Power Spectral Density Function - East-West Component

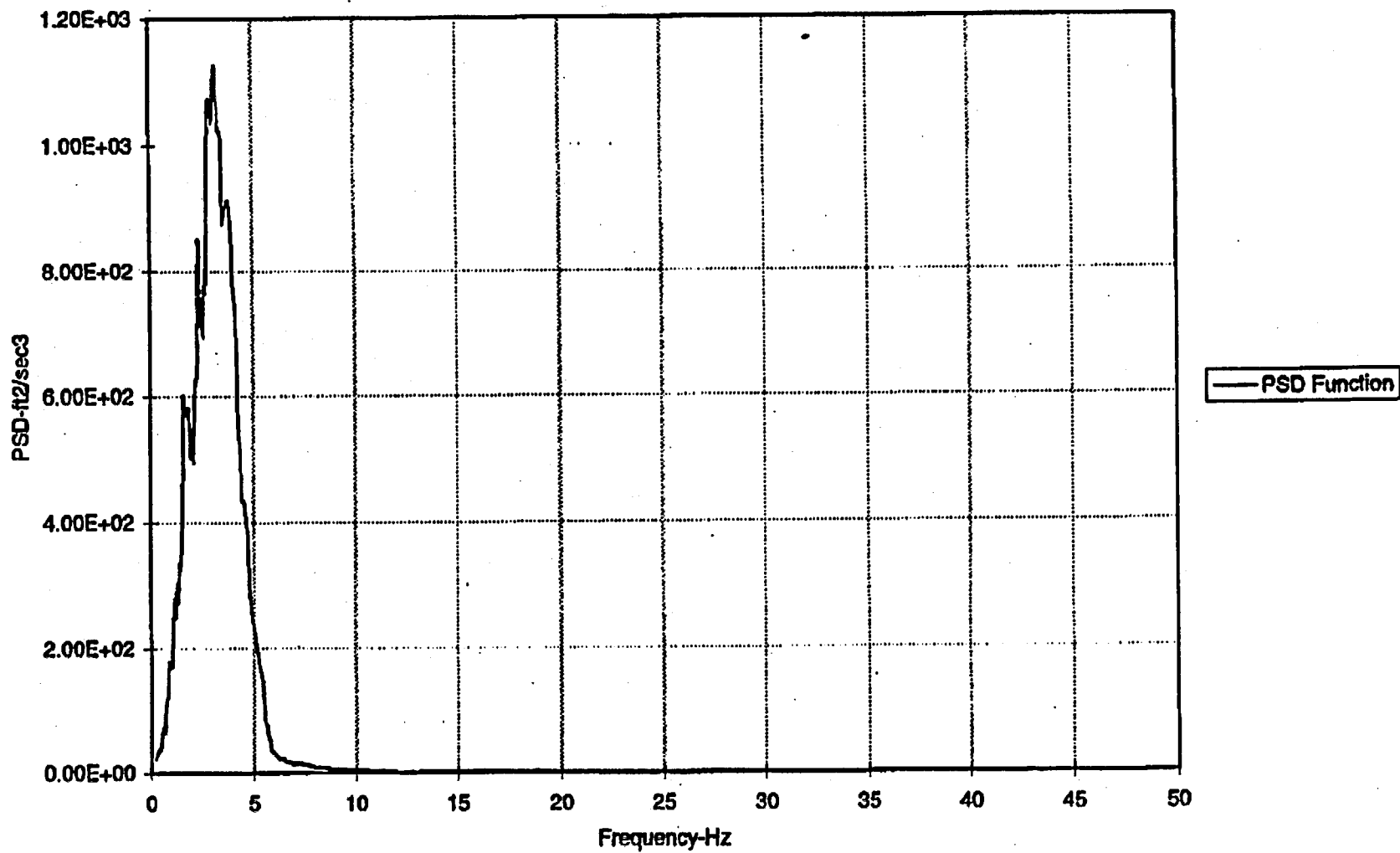


Figure 7-5: Raw Power Spectral Density Function - Vertical Component

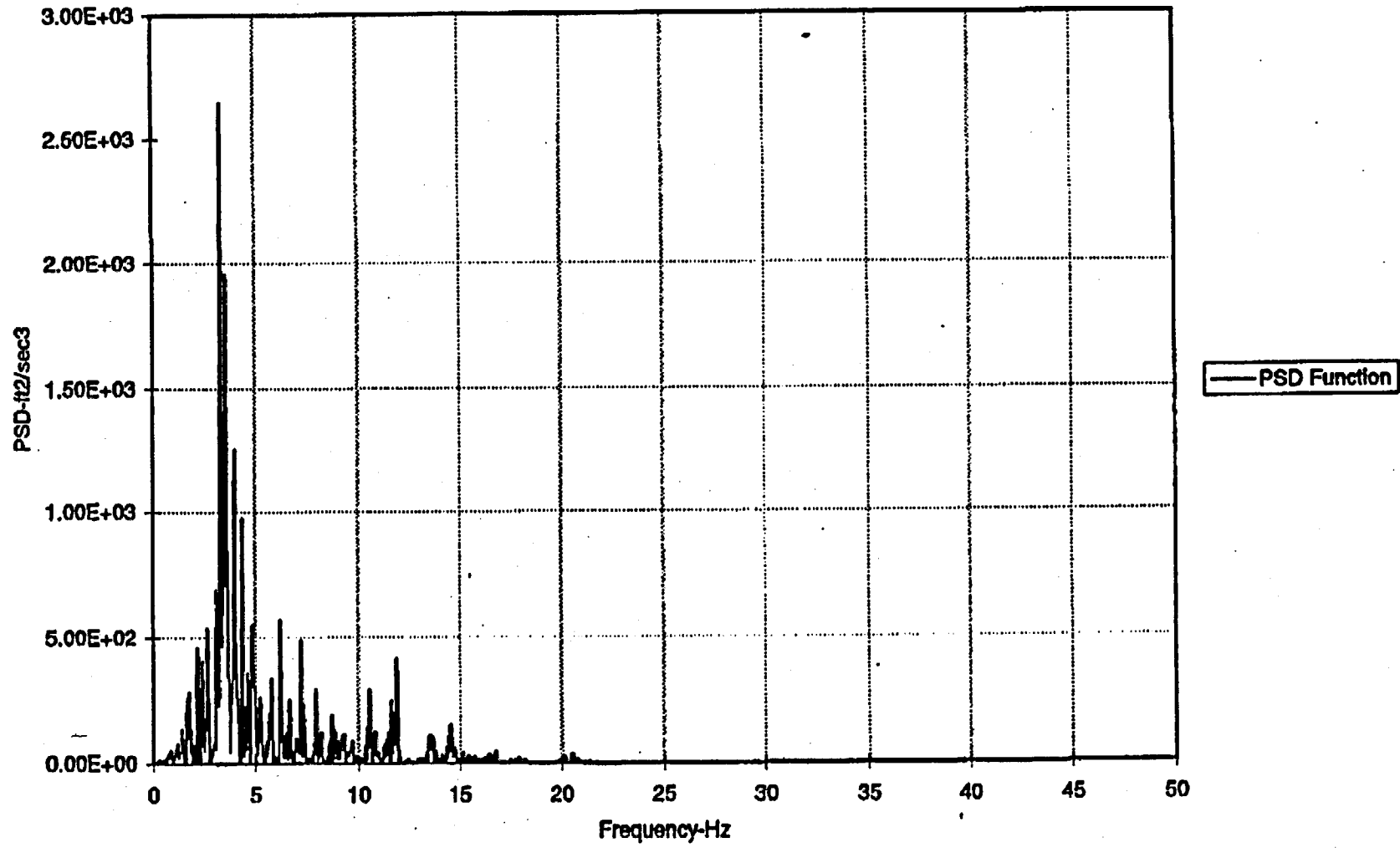
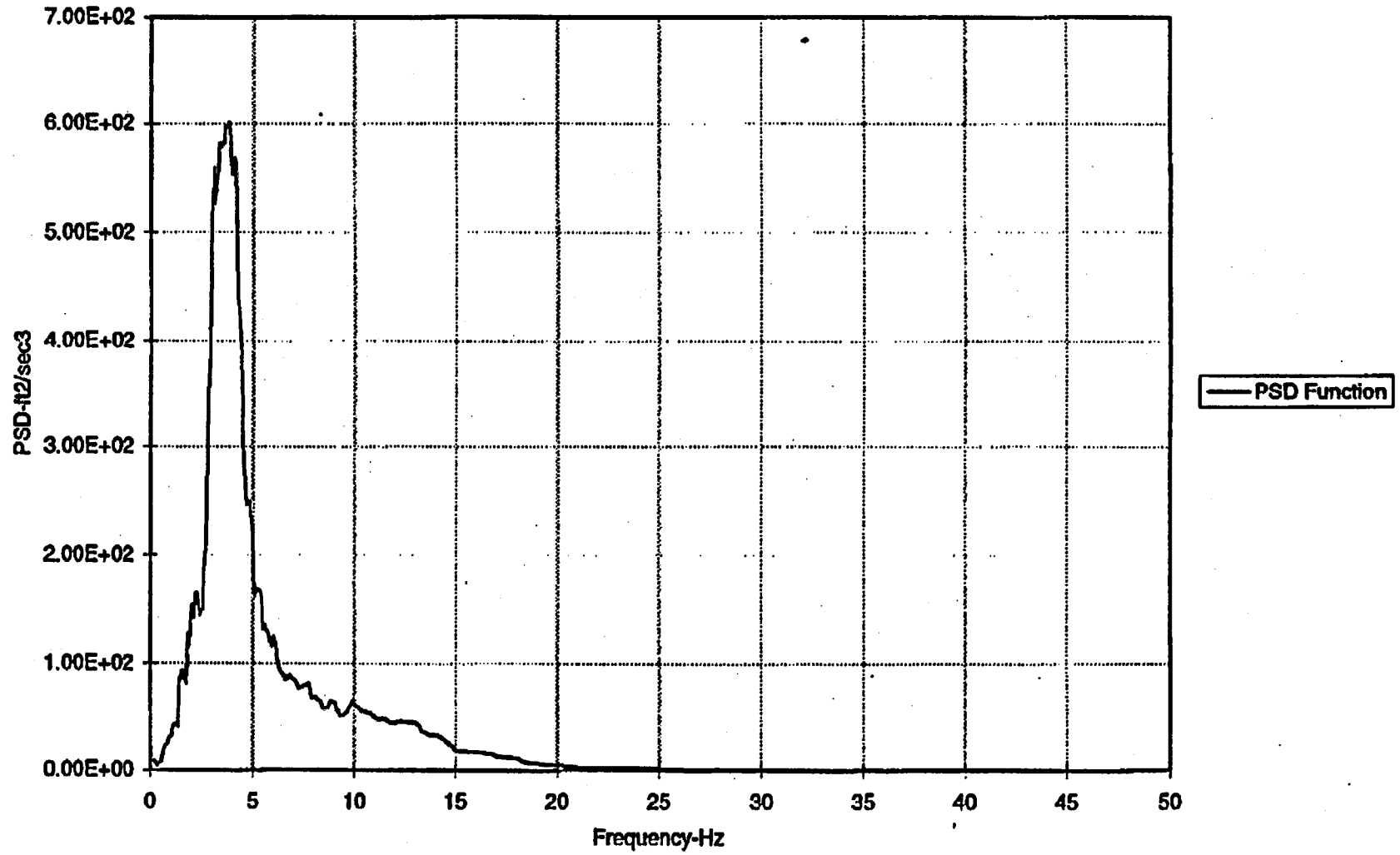


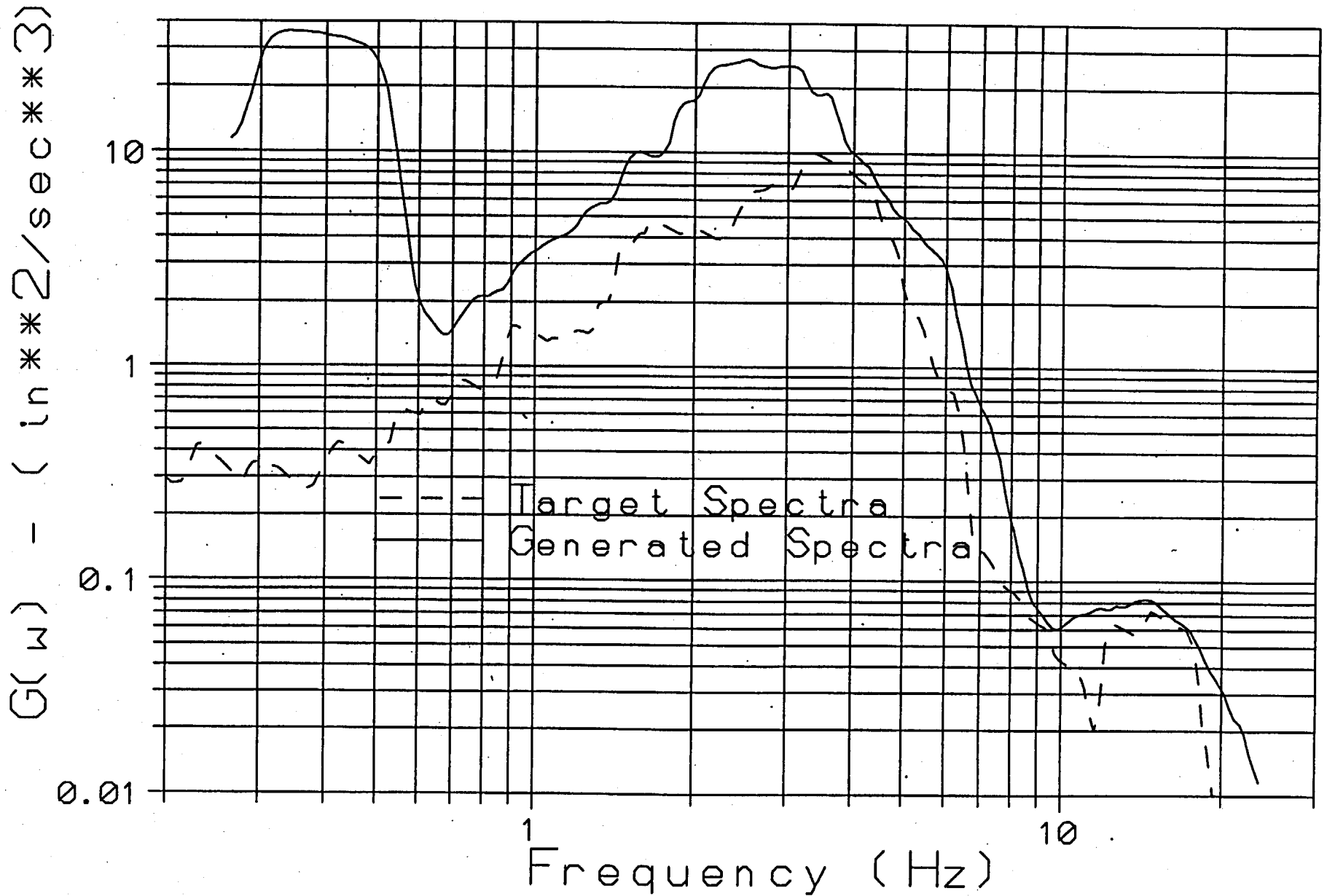
Figure 7-6: Smooth Power Spectral Density Function - Vertical Component



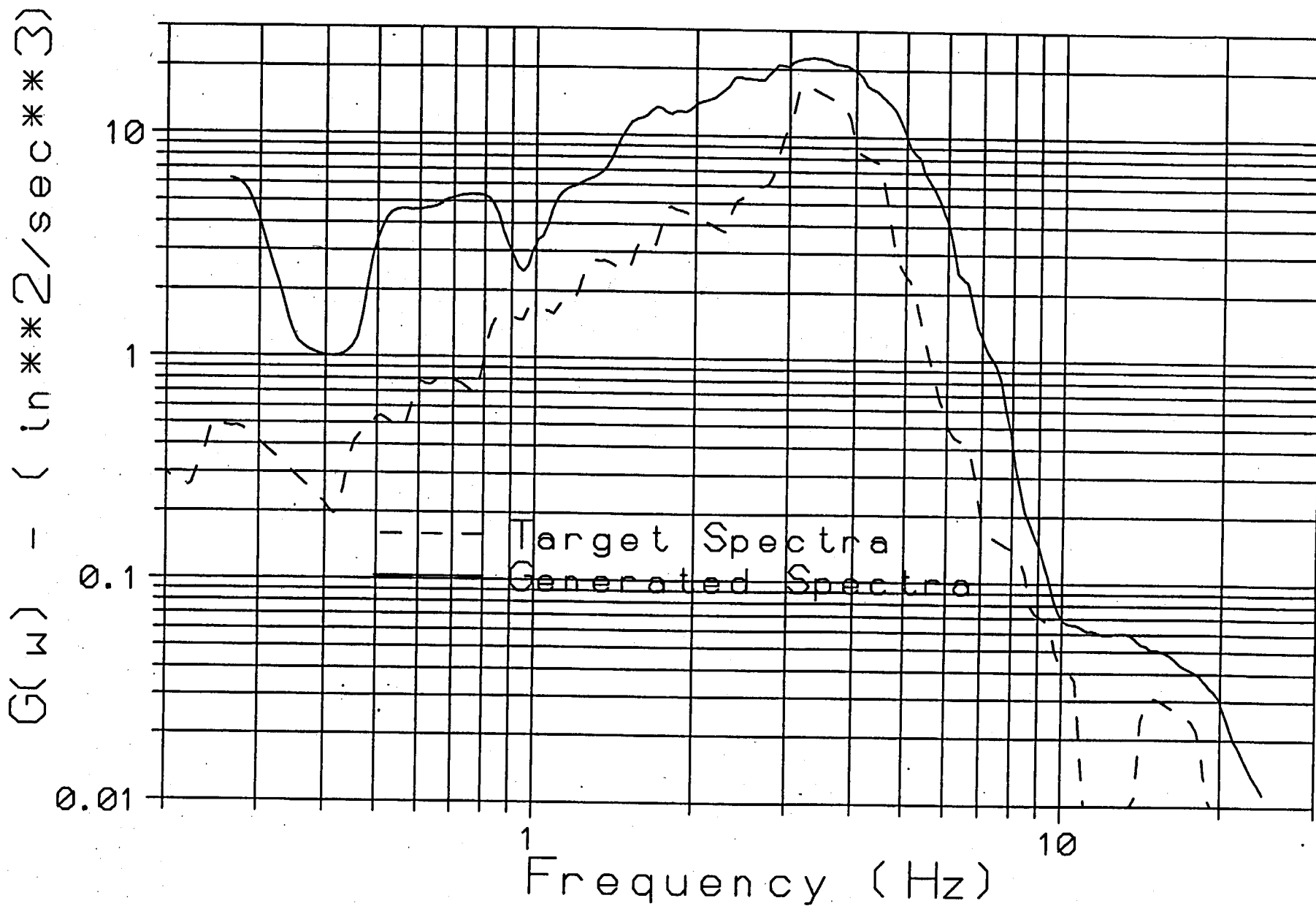
Attachment 1.5

**OCNGS OBE Time Histories at El. 75'-3"
PSD Functions Vs Targets**

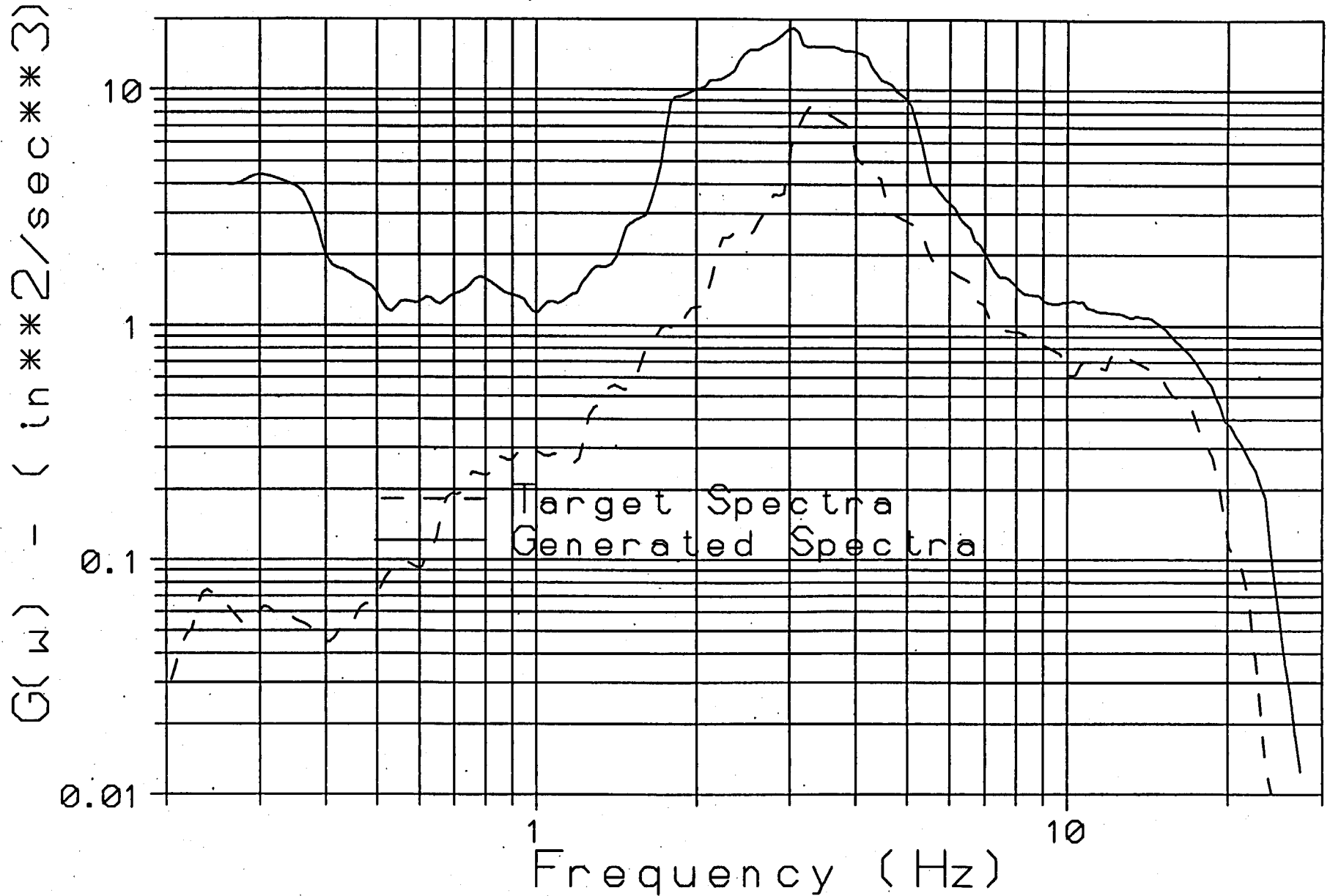
GPU Oyster Creek SFP
Power Spectral Density Function
OBE-X (NS) Direction (2% Damping) at 75'-3''



GPU Oyster Creek SFP
Power Spectral Density Function
OBE-Y (EW) Direction (2% Damping) at 75'-3''



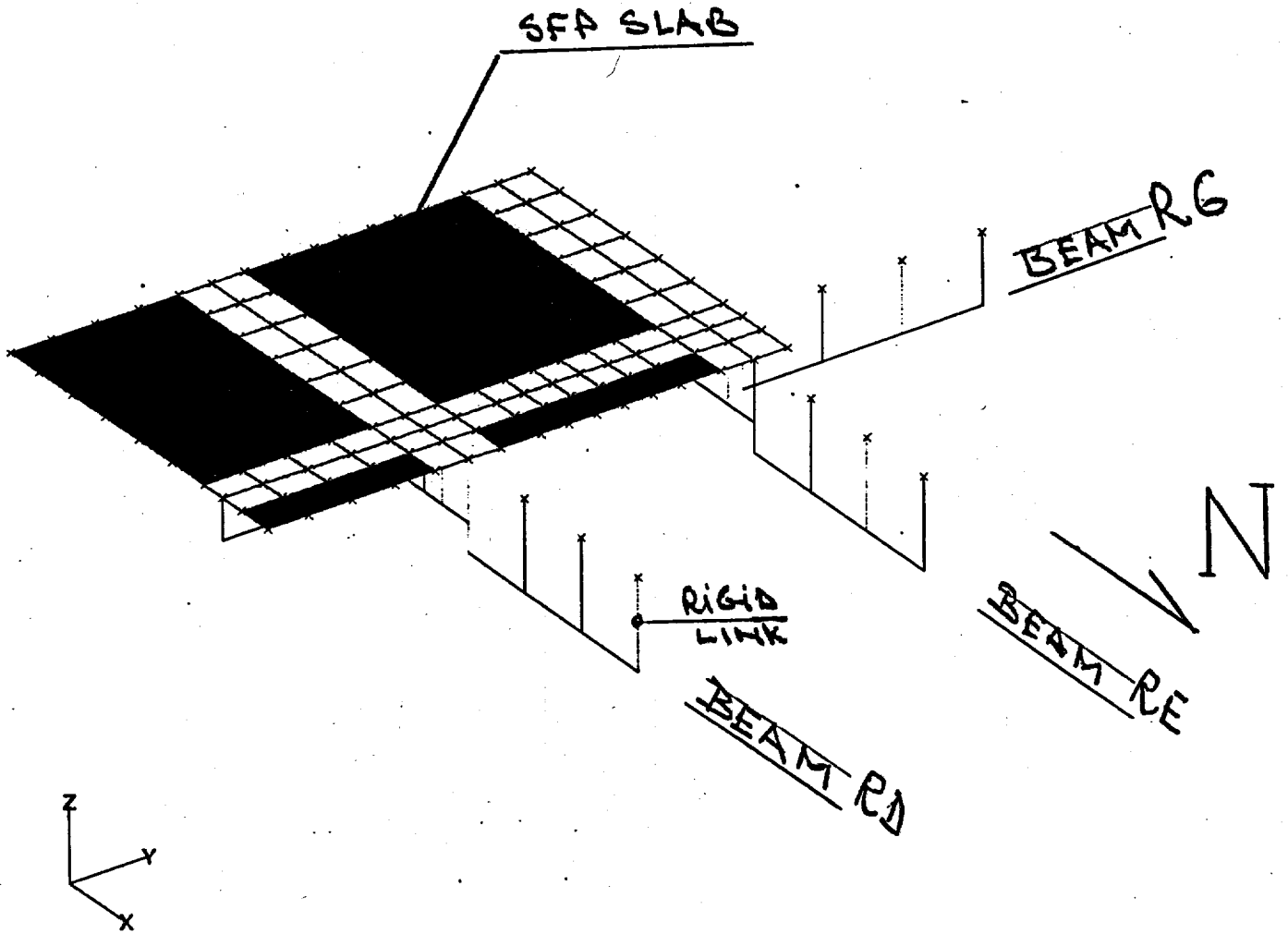
GPU Oyster Creek SFP
Power Spectral Density Function
OBE-Z (Vert) Direction (2% Damping) at 75'-3''



Attachment 2.1

Isometric View of the Finite Element Mesh

V1
L1
C1



Attachment 2.2

**Plan View of the Finite Element Mesh
W/Boundary Conditions**

Enclosure 2

- a. The stresses in the lift rods are self limiting inasmuch as an increase in the magnitude of the load reduces the eccentricity between the upward force and downward reaction (moment arm).
- b. It is impossible for a traction rod to lose engagement with the lifted rack because the downward load secures each rod in its locking slot. Moreover, the locked configuration can be directly verified from above the pool water without the aid of an underwater camera by the orientation of position locator flags atop each traction rod.
- c. A stress analysis of the rig is performed, the stress limits postulated in ANSI 14.6 (1978) are shown to be met.
- d. The rig is load tested with 300% of the maximum weight to be lifted. The test weight is maintained in the air for a minimum period of ten minutes in accordance with ANSI 14.6 (1978). All critical weld joints are liquid penetrant examined, after the load test, to establish the soundness of all critical joints.

Pursuant to the defense-in-depth approach of NUREG-0612, the following additional measures of safety will be undertaken for the reracking operation.

- a. The cranes and lifting devices used in the project will be given a preventive maintenance checkup and inspection per Oyster Creek plant procedures.
- b. Safe load paths will be developed for moving the new racks in the Reactor Building. The new racks will not be carried over any region of the pool containing fuel.
- c. The rack upending will be carried out in an area which is not poolside. Additionally, this area will not overlap any safety-related component.
- d. All crew members involved in the rack installation will be given training in the use of the lifting, upending equipment, and all other aspects of rack installation.
- e. Crane stop blocks will be temporarily installed to prevent movement over fuel.

$$\text{Dose}_v = \sum_i 0.25 (\chi/Q) F P G_i E_{v-i}$$

In this expression, G_i is the gap inventory of the gaseous radionuclides of krypton and xenon, while the $E_{\text{subscript}}$ term is the average energy per disintegration of each radionuclide (in Mev per disintegration, as given in Table 9-2). The equation assumes the noble gas decontamination factors in water and the charcoal filters are 1.0. The gap inventories of radioiodine make negligible contributions to the whole body dose, D_v , because of the large decontamination factors applicable to the iodines.

9.1.2 Results

The doses at the Oyster Creek EAB from the specified fuel handling accident are tabulated below. The doses are based on the release of all gaseous fission product activity in the gaps of all fuel rods in a highest-power assembly.

Thyroid dose, rad	=	0.483
Whole-body dose, rem	=	0.180
Skin dose, rem	=	0.685

These potential doses are well within the exposure guideline values of 10 CFR Part 100, paragraph 11. As defined in Standard Review Plan 15.7.4, *Radiological Consequences of Fuel Handling Accidents*, "well within" means 25 percent or less of the 10CFR100 guidelines, or values of 75 rad for thyroid doses and 6.25 rem for whole-body doses. The potential doses at Oyster Creek from the conservative scenario presented here meet the criteria for "well within."

9.2 Solid Radwaste

The necessity for resin replacement is determined primarily by the requirement for water clarity, and the resin is normally changed about three to four times a year. No significant increase in the volume of solid radioactive wastes is expected with the expanded storage capacity. During rack installation

Table 9-1

RESULTS OF ORIGIN CALCULATIONS FOR RADIONUCLIDES
OF IODINE, KRYPTON, AND XENON AT 100-HOURS COOLING TIME
(Extremely small values are shown as zeroes)

<u>Radionuclide</u>	<u>Curies per mtU</u>
I-131	3.836 x 10 ⁵
I-132	3.234 x 10 ⁵
I-133	4.006 x 10 ⁴
I-134	0.000 x 10 ⁰
I-135	2.731 x 10 ¹
Kr-85	1.047 x 10 ⁴
Kr-85m	2.538 x 10 ⁻²
Kr-87	0.000 x 10 ⁰
Kr-88	0.000 x 10 ⁰
Xe-131m	6.374 x 10 ³
Xe-133	7.602 x 10 ⁵
Xe-133m	1.415 x 10 ⁴
Xe-135	1.526 x 10 ³
Xe-135m	0.000 x 10 ⁰